DRAFT VERSION MARCH 8, 2024
Typeset using LaTeX **twocolumn** style in AASTeX61

arXiv:1710.05453v1 [astro-ph.HE] 16 Oct 2017

A NEUTRON STAR BINARY MERGER MODEL FOR GW170817/GRB170817A/SSS17A

A. MURGUIA-BERTHIER,[1,2] E. RAMIREZ-RUIZ,[1,2] C. D. KILPATRICK,[1] R. J. FOLEY,[1] D. KASEN,[3,4] W. H. LEE,[5] A. L. PIRO,[6] D. A. COULTER,[1] M. R. DROUT,[6] B. F. MADORE,[6] B. J. SHAPPEE,[6] Y.-C. PAN,[1] J. X. PROCHASKA,[1] A. REST,[7,8] C. ROJAS-BRAVO,[1] M. R. SIEBERT,[1] AND J. D. SIMON[6]

[1]*Department of Astronomy and Astrophysics, University of California, Santa Cruz, CA 95064, USA*
[2]*DARK, Niels Bohr Institute, University of Copenhagen, Blegdamsvej 17, 2100 Copenhagen, Denmark*
[3]*Nuclear Science Division, Lawrence Berkeley National Laboratory, Berkeley, CA 94720, USA*
[4]*Departments of Physics and Astronomy, University of California, Berkeley, CA 94720, USA*
[5]*Instituto de Astronomía, Universidad Nacional Autónoma de México, Circuito Exterior, C.U., A. Postal 70-264, 04510 Cd. de México, México.*
[6]*The Observatories of the Carnegie Institution for Science, 813 Santa Barbara Street, Pasadena, CA 91101*
[7]*Space Telescope Science Institute, 3700 San Martin Drive, Baltimore, MD 21218*
[8]*Department of Physics and Astronomy, The Johns Hopkins University, 3400 North Charles Street, Baltimore, MD 21218, USA*

ABSTRACT

The merging neutron star gravitational wave event GW170817 has been observed throughout the entire electromagnetic spectrum from radio waves to γ-rays. The resulting energetics, variability, and light curves are shown to be consistent with GW170817 originating from the merger of two neutron stars, in all likelihood followed by the prompt gravitational collapse of the massive remnant. The available γ-ray, X-ray and radio data provide a clear probe for the nature of the relativistic ejecta and the non-thermal processes occurring within, while the ultraviolet, optical and infrared emission are shown to probe material torn during the merger and subsequently heated by the decay of freshly synthesized *r*-process material. The simplest hypothesis that the non-thermal emission is due to a low-luminosity short γ-ray burst (sGRB) seems to agree with the present data. While low luminosity sGRBs might be common, we show here that the collective prompt and multi-wavelength observations are also consistent with a typical, powerful sGRB seen off-axis. Detailed follow-up observations are thus essential before we can place stringent constraints on the nature of the relativistic ejecta in GW170817.

1. INTRODUCTION

The discovery of galactic binary neutron stars (Hulse & Taylor 1975) firmly established the existence of a class of systems which would merge in less than a Hubble time via the emission of gravitational wave emission. Over the years, various studies showed that these binaries are in principle capable of powering cosmological γ-ray bursts of the short variety (Kouveliotou et al. 1993) when they merge (Paczynski 1986; Narayan et al. 1992; Eichler et al. 1989; Piran 2004; Lee & Ramirez-Ruiz 2007; Gehrels et al. 2009; Kumar & Zhang 2015), while those of the long variety have been shown to be associated to the core collapse of massive stars (Woosley & Bloom 2006). After decades of instrumental, observational and theoretical progress, a watershed event occurred on 17 August 2017, when the Swope Supernova Survey discovered the first optical counterpart of a gravitational wave event, GW170817, attributed to the merger of two neutron stars (LIGO/Virgo collaboration 2017), named SSS17a (Coulter et al. 2017). This detection led to the measurement of a redshift distance and thus the firm identification of the candidate host galaxy, NGC 4993 (Coulter et al. 2017; Pan et al. 2017).

One of the key electromagnetic discoveries concerned the detection of GRB 170817a by *Fermi* and INTEGRAL (LVC, GBM, INTEGRAL 2017; Savchenko et al. 2017), a short γ-ray burst (sGRB) lasting only a few tenths of seconds. The short duration and dim signal of the prompt γ-ray transient, however, precluded the determination of an accurate position until the Swope Supernova Survey succeeded in promptly localizing GRB 170817a/SSS17a (LVC, GBM, INTEGRAL 2017; Savchenko et al. 2017; Coulter et al. 2017). For the next few days, several multi wavelength observations were made (Savchenko et al. 2017; Haggard et al. 2017; Alexander et al. 2017; Abbott et al. 2017b). The detection of GW170817 and follow-up electromagnetic observations have revolutionized our view of merging neutron stars, confirming some previously held ideas and adding invaluable elements to our knowledge of them. The concept of a sudden release of energy almost exclusively concentrated in a brief pulse of γ-rays has been discarded. Indeed, even the term *afterglow* should be now recognized as misleading as the energy radiated during the first three weeks at longer wavelengths greatly exceeds that emitted during the prompt γ-ray phase (LVC, GBM, INTEGRAL 2017).

The broad electromagnetic manifestations of GW170817 thus provide us with a unique opportunity, to which this *Letter* is dedicated, to constrain the ejecta properties following the merger of a binary neutron star. In Section 2 we address the energetics and timescales of the observed radiation and compare it with the data from sGRBs. In Sections 3 and 4 we constrain the properties of the ejecta by using all the information available to us from both the afterglow and prompt radiation. We summarize our findings in Section 5.

2. METABOLICS OF GW170817/SSS17A

Here we construct a basic inventory of the energy radiated at all wave bands from γ-rays to radio waves using all data collected for the GW170817 event by the One-Meter Two-Hemisphere (1M2H) collaboration (Coulter et al. 2017; Drout et al. 2017; Kilpatrick et al. 2017; Shappee et al. 2017; Siebert et al. 2017) as well as from other publicly available sources (Alexander et al. 2017; Haggard et al. 2017; Savchenko et al. 2017). Such a basic inventory provides an assessment of the various modes of energy transfer and release involved within the ejecta. The compilation also offers a way to test our understanding of the physics of neutron star mergers. Some apparent points should be emphasized. We measure directly only the the energy radiated in the direction of the Earth per second per steradian per frequency interval by the source. The apparent bolometric luminosity $L_{\rm iso}$ may be quite different from the true bolometric luminosity if the source is not isotropic. To investigate the energy dissipation history we fitted a natural cubic spline function to the luminosity $L_{\rm iso}$ as a function of time at different frequency intervals. This allows us to estimate the cumulative emitted energy $E_{\rm iso}$ and also derive t_{90} values at all energies, which we define here as the time in the source frame during which 90% of the radiated energy is accumulated. Using this, we derive $E_{\rm iso}$ and t_{90} at γ-ray (75-2000 keV) from Abbott et al. 2017b, X-ray (0.3-10 keV), ultraviolet (2600-3465 Å), optical (3465-9665 Å), infrared (10200-21900 Å) and radio (5-10 GHz) energies:

- $E_{\gamma,\rm iso} \approx 5.3 \pm 1.1 \times 10^{46}$ erg and $t_{90,\gamma} \approx 2$ s
- $E_{\rm IR,iso} \approx 2.7 \pm 0.5 \times 10^{48}$ erg and $t_{90,\rm IR} \approx 10.5$ days
- $E_{\rm O,iso} \approx 4.1 \pm 0.4 \times 10^{47}$ erg and $t_{90,\rm O} \approx 3.8$ days
- $E_{\rm UV,iso} \approx 1.3 \pm 0.6 \times 10^{47}$ erg and $t_{90,\rm UV} \approx 1.1$ days
- $E_{\rm X,iso} \approx 1.9 \pm 0.5 \times 10^{44}$ erg and $t_{90,\rm X} \gtrsim 15.2$ days
- $E_{\rm R,iso} \lesssim 8 \times 10^{40}$ erg and $t_{90,\rm R} \gtrsim 17.7$ days

While unremarkable for its duration, GRB 170817a had a total energy that is some 4-6 orders of magnitude less than a typical *Swift* sGRB (Gehrels et al. 2009). The currently inferred isotropic X-ray emission $E_{\rm iso,X}$, which for most *Swift* sGRBs is comparable to that emitted during the prompt γ-ray phase, is at least 6-8 orders of magnitude smaller (Gehrels et al. 2009). The isotropic equivalent energy that is radiated at optical wavelengths in this case is 2 orders of magnitude larger than that in γ-rays. This is in stark contrast to *Swift* sGRBs, for which $E_{\rm O,iso}$ is at least 2 orders of magnitude

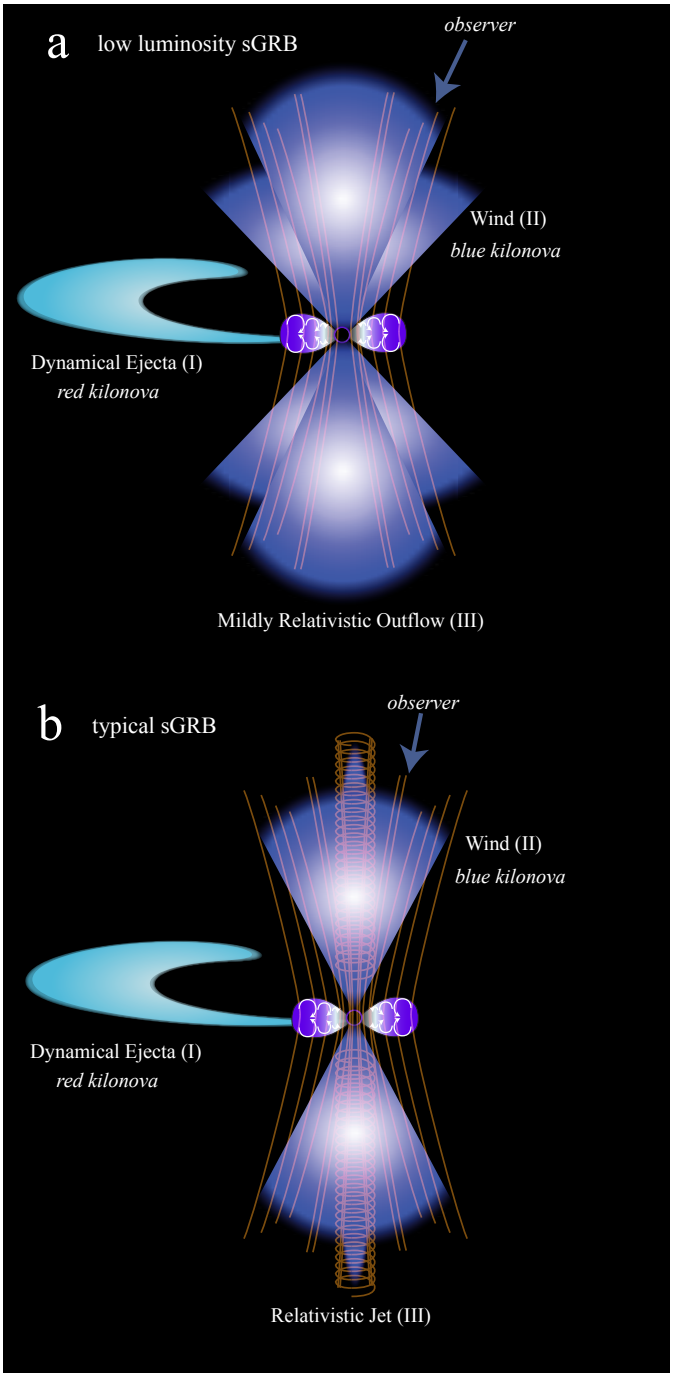


Figure 1. An overview of the main energy transfer processes thought to be involved in ejecting material in neutron star mergers. As they merge a few percent of the matter is ejected in the form of a tidal tail (I). The shocked merged remnant is expected to produce strong winds (II) and is likely to be top-heavy and unable to survive. The expected outcome is the collapse to a black hole. A spinning black hole constitutes an excellent gyroscope, and the ingredients of accretion and magnetic fields are probably sufficient to ensure the production of a sGRB jet (III in scenario *b*). A potential death-trap for such highly relativistic outflows is the amount of entrained baryonic mass, which can severely limit their power (III in scenario *a*).

smaller than $E_{\gamma,\rm iso}$. What is more, GW170817/SSS17a is radically different in its optical properties from any other known sGRBs (Siebert et al. 2017). The optical emission rises in less than half a day, then fades rapidly, exhibiting a swift color evolution to redder wavelengths (Drout et al. 2017). While optical sGRB afterglows can produce rapidly fading transients, they don't generate the quasi-blackbody spectrum that is observed in SSS17a (Shappee et al. 2017). These results are consistent with the emerging hypothesis that the ultraviolet, optical and infrared emission probe matter torn from the merger system, ejected at sub-relativistic velocities and subsequently heated by the decay of freshly synthesized *r*-process material (Kilpatrick et al. 2017; Kasen et al. 2017).

On its own, the low-luminosity γ-ray emission of the unusually faint GRB 170817a can thus support the idea of a common class of intrinsically sub-energetic sGRBs. The key question is whether there is significant observational support for the existence of low amounts of relativistic energy released during this event or whether the afterglow light curves are instead more consistent with a model in which GRB 170817a was a classical jetted sGRB viewed off-axis. Figure 1 presents here our selections for the energy transfer channels during merging neutron star binaries that we believe are responsible for the various entries in the inventory. Material dynamically stripped during the merger (denoted I in Figure 1) is ejected by tidal torques through the outer Lagrange point, removing energy and angular momentum and forming a large tidal tail (Kluźniak & Lee 1998; Rosswog 2005; Faber & Rasio 2012). This material is expected to undergo *r*-process nucleosynthesis and give rise to a red (quasi-thermal) kilonova (Li & Paczyński 1998; Freiburghaus et al. 1999; Metzger et al. 2010; Roberts et al. 2011). The configuration after merger consists of a hyper massive neutron star (HMNS, one with more mass than a cold, non-rotating configuration could support) surrounded by an extended shock-heated envelope (Baumgarte et al. 2000; Duez et al. 2006). During this stage, various dissipation and transport mechanisms can give rise (Perego et al. 2014; Siegel et al. 2014) to strong winds (denoted II in Figure 1). These are thought to produce low-opacity (first-peak) *r*-process material, giving rise to a blue (quasi-thermal) kilonova (Kasen et al. 2013, 2015; Metzger & Zivancev 2016). The properties of the HMNS have a decisive outcome on whether or not a standard sGRB will be observed (Murguia-Berthier et al. 2014, 2017; Piro et al. 2017). This is because even a tiny mass of baryons polluting the jet will severely limit the maximum attainable Lorentz factor and effective jet triggering might have to wait until after black hole collapse. In scenario *a*, the wind emanating from the HMNS hampers the advancement of a relativistic jet, leading to a low luminosity event (Rosswog & Ramirez-Ruiz 2002, 2003; Nagakura et al. 2014; Just et al. 2016). In scenario *b* in Figure 1, the collapse to a black hole occurs

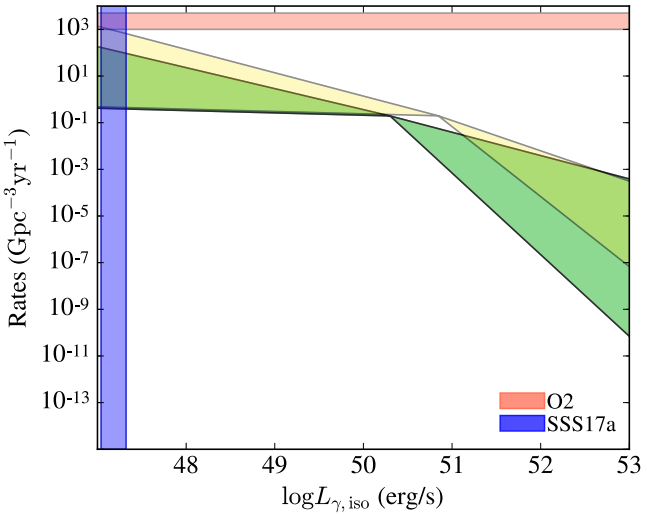


Figure 2. Shown are two luminosity functions taken from Guetta & Piran 2006. They are described by a broken power-law peak luminosity function with $L_* = 0.2 \times 10^{51}$ erg/s, $a = 0.6^{+0.3}_{-0.5}$, $b = 1.5^{+2}_{-0.5}$ (green) and $L_* = 0.7 \times 10^{51}$ erg/s, $a = 0.6^{+0.4}_{-0.5}$, $b = 2^{+1}_{-0.7}$ (yellow). If we assume a beaming correction factor of 27^{+158}_{-18} we find a merger rate that is broadly consistent with estimated O2 LIGO rates Abbott et al. 2016 and can accommodate the $L_{\gamma,\rm iso}$ measured by LVC, GBM, INTEGRAL 2017 for GW170817/SSS17a/GRB 170817a.

promptly and a classical jetted sGRB is produced which we happen to view off-axis (such as Ramirez-Ruiz et al. 2005). Not only would a sGRB be detectable in both scenarios, followed by an afterglow, but there could also be additional extended emission at early stages caused by the reprocessing of this energy and its subsequent dissipation (Murguia-Berthier et al. 2014; Rezzolla & Kumar 2015). This could resemble the so called extended emission in sGRBs (Norris & Bonnell 2006). In the following sections, we examine these two possible interpretations and critically asses whether the electromagnetic observations of GW170817/SSS17a support the idea that it was an intrinsically weak, nearly isotropic explosion or either a classical sGRB, such as GRB 130603b (Fong et al. 2015), observed off-axis. An accurate assessment of the kinetic energy content in relativistic material requires detailed afterglow modeling.

3. A LOW LUMINOSITY SGRB

GW170817/SSS17a/GRB 170817a, or at least the γ-ray emission along our line of sight, was certainly feeble. The simplest interpretation might be that the γ-ray emission was deficient in all directions (scenario *a* in Figure 1), as in the case of low luminosity long GRBs associated with type Ic supernovae (Kaneko et al. 2007).

Such a weak burst, thousands to millions of times fainter than the inferred isotropic energies of sGRB, could belong to a separate population of weakly jetted, low luminosity events. We thus need to quantify the odds of detecting such an event as non-Euclidean number count statistics limit the fraction of bursts that can be observed from the local Universe (Bloom et al. 1998).

In Figure 2 we compare the properties of GRB 170817a (LVC, GBM, INTEGRAL 2017) with the luminosity function of sGRBs as constrained from the peak flux distribution of BATSE events and the redshift and luminosity distributions of *Swift* events. The luminosity functions shown in Figure 2 have been derived (Guetta & Piran 2006) under the assumption that the sGRB rate follows a distribution of delay times that is consistent with those commonly used to describe the merging rate of double neutron star binaries (Champion et al. 2004; Behroozi et al. 2014; Shen et al. 2015).

If we assume a typical beaming correction of 27^{+158}_{-18} for sGRBs (Fong et al. 2015), we find an event rate that is broadly consistent with the O2 LIGO merger rate estimated by Abbott et al. 2016 and can accommodate the $L_{\gamma,\rm iso}$ measured by LVC, GBM, INTEGRAL 2017, under the assumption that GRB 170817a was similarly weak in all directions. BATSE was a benchmark experiment that produced a catalogue containing more than 2,000 GRBs (Paciesas et al. 1999). How many of these bursts could have been GW170817-like events? The observed number of sGRBs and the lack of excess events from the direction of the Virgo cluster suggests that only a tiny fraction ($\lesssim 0.05$) of these bursts can be like GW170817 within $\lesssim 40$ Mpc (Palmer et al. 2005).

3.1. *Prompt Emission*

The energy spectrum for GRB170817a is well described by a power law with an exponential cutoff at ≈ 185 keV (LVC, GBM, INTEGRAL 2017). With no significant emission observed above 300 keV, GRB170817a is an example of the *no high-energy* bursts that compose 25% of the BATSE sample (Paciesas et al. 1999). Since GRB 170817a had a single-peaked light curve (LVC, GBM, INTEGRAL 2017), the burst variability, $\delta t_{\rm var}$, is roughly given by $\delta t_{\rm var} \approx t_{90,\gamma} \approx 2 \pm 0.5$s (Abbott et al. 2017b).

A constraint on the size of the emitting region R_γ can be derived from the delay time $\delta t_{\rm gw} \approx t_{90,\gamma} \approx 2$s (Abbott et al. 2017b) observed between the arrival of the prompt γ-ray emission and the gravitational wave merger signal. If one assumes that the relativistic outflow, moving at $\Gamma = (1-\beta^2)^{-1/2}$, was triggered at merger, then

$$R_\gamma = c\delta t_{\rm gw}\beta(\beta-1)^{-1} \approx 2\Gamma^2 c\delta t_{\rm gw},$$

which is consistent with most studies aimed at understanding the nature of the γ-ray dissipation in sGRBs (Nakar 2007; Kumar & Zhang 2015). Internal shocks dissipation, for example, is thought to occur at a radius $R_\iota \approx 2\Gamma^2 c\delta t_{\rm v}$ (Rees & Meszaros 1992). Since $\delta t_{\rm var} \approx \delta t_{\rm gw}$, it follows that $R_\iota \approx R_\gamma$.

3.2. *The Afterglow Emission*

If there was indeed this amount of relativistic energy we can then try to explain why we did not see the afterglow emission at early times by invoking a standard afterglow model. In such quasi-spherical case, the emission we expect should be below the ultraviolet, optical and infrared emission, which is dominated by heating from the decay of freshly synthesized r-process material (Coulter et al. 2017; Drout et al. 2017; Kilpatrick et al. 2017; Shappee et al. 2017; Siebert et al. 2017).

The resulting light curves for a low energy spherical model are plotted against observations of SSS17a in Figure 3. As a point of comparison, we plot the light curves of GRB 130603b, whose afterglow properties are representative of classical sGRBs (Fong et al. 2015). The local emissivity is calculated using standard assumptions of synchrotron emission from relativistic electrons that are accelerated behind the shock (with a power-law distribution of energies wind index p) where the magnetic field and the accelerated electrons hold fractions ϵ_e and ϵ_B, respectively, of the internal energy.The model parameters are: $n = 0.08$ cm^{-3}; $E_{\rm K,iso} = 8 \times 10^{48}$ erg, $p = 2.1$, $\epsilon_B = 0.05$, $\epsilon_e = 0.05$ and the fraction of electrons that get accelerated is $\xi_N = 1$. We emphasize that the model parameters cannot be uniquely determined from the fit to the multi-wavelength observations, and other sets of parameters could provide an equally acceptable description. The X-ray emission is very sparsely sampled and thus provide only mild constraints on models on its own. However, when combined with the optical and radio limits, they provide a better handle on the model, thus significantly improving upon the constraints derived from the X-ray data alone. The reader is refer to Kumar & Zhang 2015 for a detailed description of our current understanding regarding afterglow physics and observational constraints.

The fact that X-ray emission was seen at $t = 15.2$ days, implies that $t_{\rm dec} \lesssim 15.2$ days, where $t_{\rm dec} = R_{\rm dec}/(2c\Gamma^2)$ and $R_{\rm dec} = (3E_{\rm k,iso}/4\pi n m_p c^2 \Gamma^2)^{1/3}$ are the observed time and radius at which the outflow decelerates appreciably (Piran 2004). In the model depicted in Figure 3, the initial Lorentz factor of the blast wave is chosen to be $\Gamma = 5.5$ in order for $t_{\rm dec} \lesssim 15.2$ days. In this case, $R_\gamma \approx 3.6 \times 10^{12} (\Gamma/5.5)^2 (\delta t_{\rm gw}/2{\rm s})$ cm.

Some points from should be emphasized here. The afterglow light curves provide a reasonable description of the sparsely sampled X-ray afterglow and are consistent with the lack of non-thermal radiation observed at radio and optical wavelengths. The optical emission is dominated by quasi-thermal emission, which also dominates the total radiated energy output (Drout et al. 2017). This is illustrated in Figure 3, where the best fit models for the kilonova emission at optical wavelengths are plotted. These models have been constructed using the simple formalism developed by Metzger 2017 and are tailored to match the values derived in Kilpatrick et al. 2017 using more sophisticated models. In this

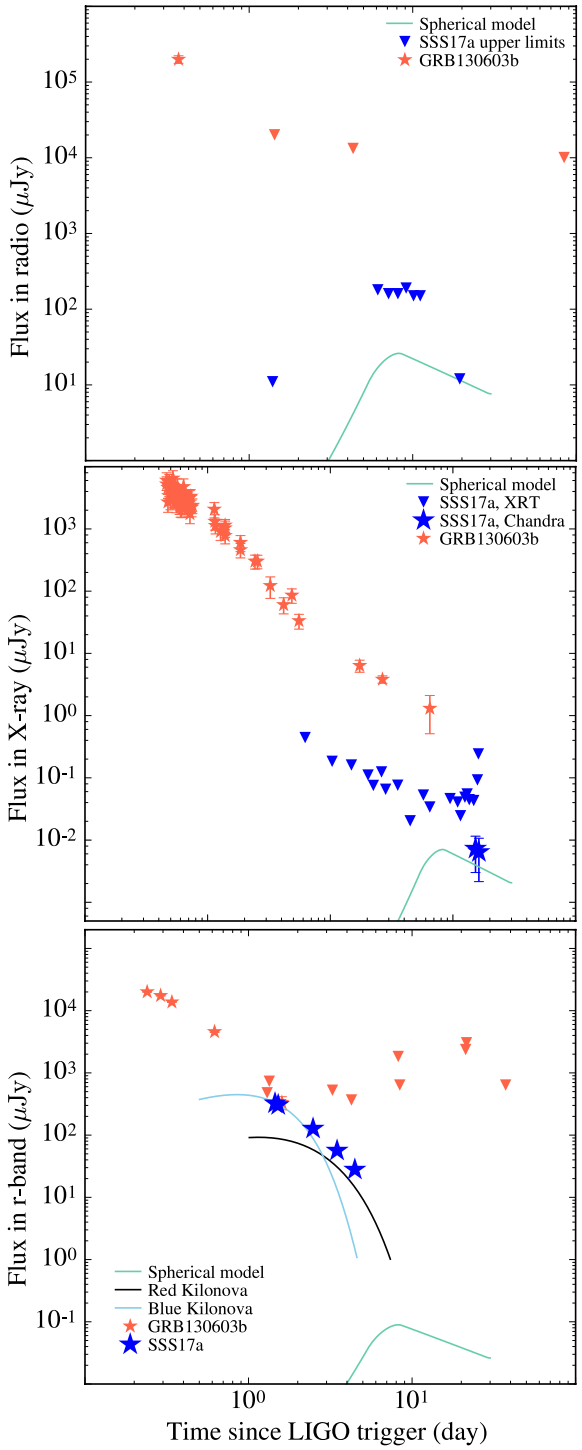


Figure 3. Afterglow emission from a spherical, low energy blast wave (scenario *a* in Figure 1) at optical (r-band), radio (6 GHz), and X-rays (7×10^{16} Hz). The afterglow light curves presented here are calculated using the blast wave models from Leventis et al. 2012. The microphysical parameters, the energetics and the properties of the external medium and burst energetics are given in the text. Also plotted is data from the One-Meter Two-Hemisphere collaboration: Coulter et al. 2017; Drout et al. 2017; Kilpatrick et al. 2017; Shappee et al. 2017; Siebert et al. 2017 for the r-band, Haggard et al. 2017 for the X-rays, and Alexander et al. 2017, EuroVLBI team for the radio. The afterglow detections and upper-limits of the standard GRB 130603b are plotted for comparison (Fong et al. 2015).

simple model, we contemplate ejecta of mass $m_{\rm ejecta}$ expanding at a velocity $v_{\rm ejecta}$, which is heated by the decay of freshly synthesized r-process material. Two different ingredients are assumed for the ejecta: a *blue* ($m_{\rm ejecta} = 0.025 M_\odot$ and $v_{\rm ejecta} = 0.3c$) and a *red* ($m_{\rm ejecta} = 0.035 M_\odot$ and $v_{\rm ejecta} = 0.15c$) component. We use $\kappa_{\rm blue} = 0.08$ cm^{2}g^{-1} and $\kappa_{\rm red} = 5$ cm^{2}g^{-1} to describe the opacity of the blue (lanthanide free) and red (lanthanide rich) components, respectively (Barnes & Kasen 2013). This two component model, as argued in Kilpatrick et al. 2017, is in remarkable agreement with the wealth of observations our team has assembled at optical, ultraviolet and infrared wavelengths (Coulter et al. 2017; Drout et al. 2017; Kilpatrick et al. 2017; Shappee et al. 2017; Siebert et al. 2017). What is more, observations at γ-rays, X-rays and radio wavelengths are consistent with GRB 170817a being an intrinsically weak, nearly isotropic explosion. Having said this, continuous monitoring of the source at X-ray and radio wavelengths could render this type of model unacceptable if the integrated energy is observed to increase.

4. AN OFF-AXIS MODEL

Given that most sGRBs are collimated (Fong et al. 2015), their observed properties will unavoidably change depending on the angle $\theta_{\rm obs}$ (measured with respect to the jet axis) at which they are observed. If we make the standard assumption of a top-hat jet, the prompt and afterglow properties of the sGRB would be almost the same to all observers located within the initial jet aperture, denoted here as θ_0. At $\theta_{\rm obs} > \theta_0$, the jet emission is expected to decline precipitously (Granot et al. 2002).

4.1. *Prompt Emission*

In a typical sGRB (scenario *b* in Figure 1), the γ-rays we detect are concentrated into a cone of opening angle comparable to θ_0, provided that $\theta_0 > \Gamma^{-1}$. Thus, if the jet is viewed at $\theta_{\rm obs} > \theta_0$ from the jet axis, the γ-ray luminosity will be drastically suppressed. For a jet with Γ, the typical peak photon energy $E_{\rm p}$ scales as (Ramirez-Ruiz et al. 2005)

$$E_{\rm p} \propto [\Gamma(\theta_{\rm obs} - \theta_0)]^{-2},$$

while

$$E_{\gamma,{\rm iso}} \propto [\Gamma(\theta_{\rm obs} - \theta_0)]^{-6}.$$

Figure 4 shows a sample of observed $E_{\rm p}$ and $E_{\gamma,{\rm iso}}$ for sGRBs together with the properties of GRB 170817a if it were viewed on-axis. In order to generate the on-axis conditions we have used $\theta_{\rm obs} = 1.5\theta_0$ and $\theta_0 = 0.2$, which we inferred from a fit to the afterglow emission (see Section 4.2 for details), and have assumed $\Gamma = 50$. These values are compatible with those observed in (and in some cases derived for) sGRBs (Gehrels et al. 2009; Berger 2014; Fong et al. 2015). We thus consider $\Gamma = 50$ and the inferred on-axis values of

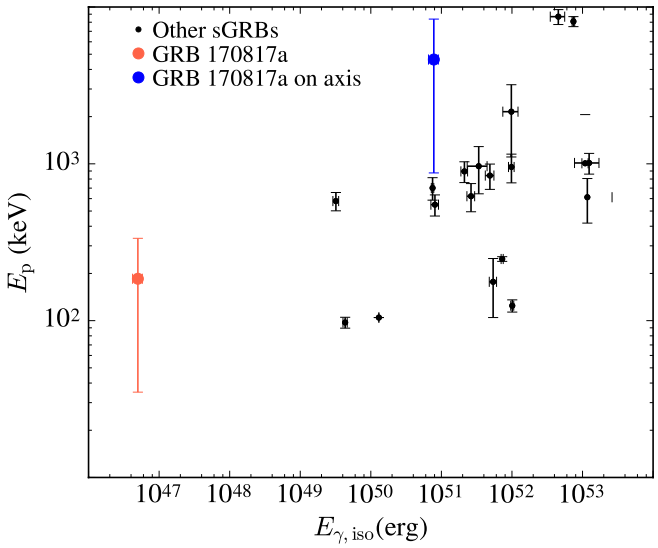


Figure 4. The location of GRB 170817a in the $E_{\rm p}$ and $E_{\gamma,{\rm iso}}$ plane, from Savchenko et al. 2017; LVC, GBM, INTEGRAL 2017. Also shown is the location if GRB 170817a were on-axis under the assumption of a misaligned, sharp-edged jet. This assumes a Lorentz factor of $\Gamma \approx 50$ and $\Gamma(\theta_{\rm obs} - \theta_0) \approx 5$ (Section 4.2). The data for the other sGRBs are taken from Tsutsui et al. 2013 and D'Avanzo et al. 2014.

$E_{\rm p} \approx 4$ MeV and $E_{\gamma,{\rm iso}} \approx 7 \times 10^{50}$ erg to be reasonable for conditions expected at the edge of the jet (Ramirez-Ruiz et al. 2005).

For $\theta_{\rm obs} > \theta_0$, one expects some significant decrease in the variability of the prompt emission. This is because the duration of an individual pulse in the light curve scales as $\delta t_{\rm var} \propto [\Gamma(\theta_{\rm obs} - \theta_0)]^2$. Since the distance between neighboring pulses is typically comparable to the width of an individual pulse, then a sizable increase in $\delta t_{\rm v}$ could cause significant overlap between pulses and, as a result, the variability would be washed out.

The total duration of the event could also increase significantly for large viewing angles when $[\Gamma(\theta_{\rm obs} - \theta_0)]^2 \gtrsim (t_{90,\gamma}/\delta t_{\rm var})$, where the total observed duration of the burst ($t_{90,\gamma}$) and individual pulse variability ($\delta t_{\rm var}$) are measured here on-axis. For most sGRBs, $(t_{90,\gamma}/\delta t_{\rm var}) \approx 10 - 10^2$ (Gehrels et al. 2009), which implies that for $[\Gamma(\theta_{\rm obs} - \theta_0)]^2 < t_{90,\gamma}/\delta t_{\rm var} \sim 10 - 10^2$ the total duration of the burst when observed off-axis should not increase significantly. The variability of the burst, when observed off-axis on the other hand, is expected to be smeared out.

Based on the model parameters estimated here, we thus expect GRB170817a to have been significantly more luminous, have a shorter duration, be more variable and have a much harder spectrum for observers located within $\theta_{\rm obs} \lesssim \theta_0$. This might explain why GRB170817a was observed to be somewhat less variable than typical sGRBs. As argued in Section 3.1, the observed time delay between the arrival of the

gravitational wave signal and the prompt γ-ray emission can be used to place constraints on the size of the emitting region although the degree of pulse and light curve smearing in this scenario complicates the calculation.

4.2. *Afterglow Emission*

An observer at $\theta_{\rm obs} > \theta_0$ observes a rising afterglow light curve at early times (Granot et al. 2002). The afterglow light curve will be observed to peak when Γ, which is decreasing with time, reaches a value $\approx (\theta_{\rm obs} - \theta_0)^{-1}$ and soon after will approach that seen by an on-axis observer. This can be discerned by comparing the curves for $\theta_{\rm obs} = \theta_0$ and $\theta_{\rm obs} = 2\theta_0$ in Figure 5. The observations of GRB 170817a/SSS17a can be accommodated if $\theta_{\rm obs} \approx 1.5\theta_0$ for $\theta_0 = 0.2$. That is, our line of sight happened to be a few degrees from a sharp-edged typical sGRB jet. The constraints inflicted by the properties of the afterglow emission thus support the idea that GRB 170817a/SSS17a was a standard sGRB jet seen off-axis. The on-axis model $\theta_{\rm obs} \lesssim \theta_0$ in this case provides a reasonable description of the broad afterglow properties of GRB 130603b (Fong et al. 2015), which by all accounts is representative of the sGRB population. The isotropic kinetic energy of the jet, when viewed on axis, would be $E_{\rm K,iso} = 2.5 \times 10^{51}$ erg, which can explain (for reasonable dissipation efficiencies) $E_{\gamma,\rm iso}(\theta_{\rm obs} \lesssim \theta_0)$ in Figure 4. The simple off-axis fit to the afterglow observations does not, however, uniquely determine the model parameters. Some model constraints are, however, rather robust. Most notably within the framework presented here, if the jet axis had been closer to the observer's direction, the intensity of the optical and infrared afterglow might have prevented us from uncovering the kilonova signal. This can be clearly seen by comparing the properties of SSS17a with those of GRB 130603b. This implies that the edge of the jet must be sufficiently sharp, so that the emission at early times would be dominated by the core of the jet, rather than by material along the line of sight that might produce bright radio, optical and X-ray emission.

5. CONCLUSION AND PROSPECTS

The recent discovery of GRB 170817a/SSS17a associated with GW170817 (Coulter et al. 2017; LVC, GBM, INTEGRAL 2017) has made it possible to strengthen the case for binary neutron star mergers as the main progenitors of sGRBs (Piran 2004; Lee & Ramirez-Ruiz 2007; Nakar 2007; Gehrels et al. 2009; Rezzolla et al. 2011; Berger 2014). While the isotropic energy emitted in gravitational waves is of the order of a fraction of a solar rest mass $\gtrsim 0.025 M_\odot c^2 \approx 4.5 \times 10^{52}$ erg (Abbott et al. 2017a), the total integrated electromagnetic emission is estimated here to be drastically lower $\approx 5 \times 10^{48}$ erg (Section 2) and was dominated by the quasi-thermal emission seen at infrared, optical and ultraviolet wavelengths. By modeling this emission in great detail,

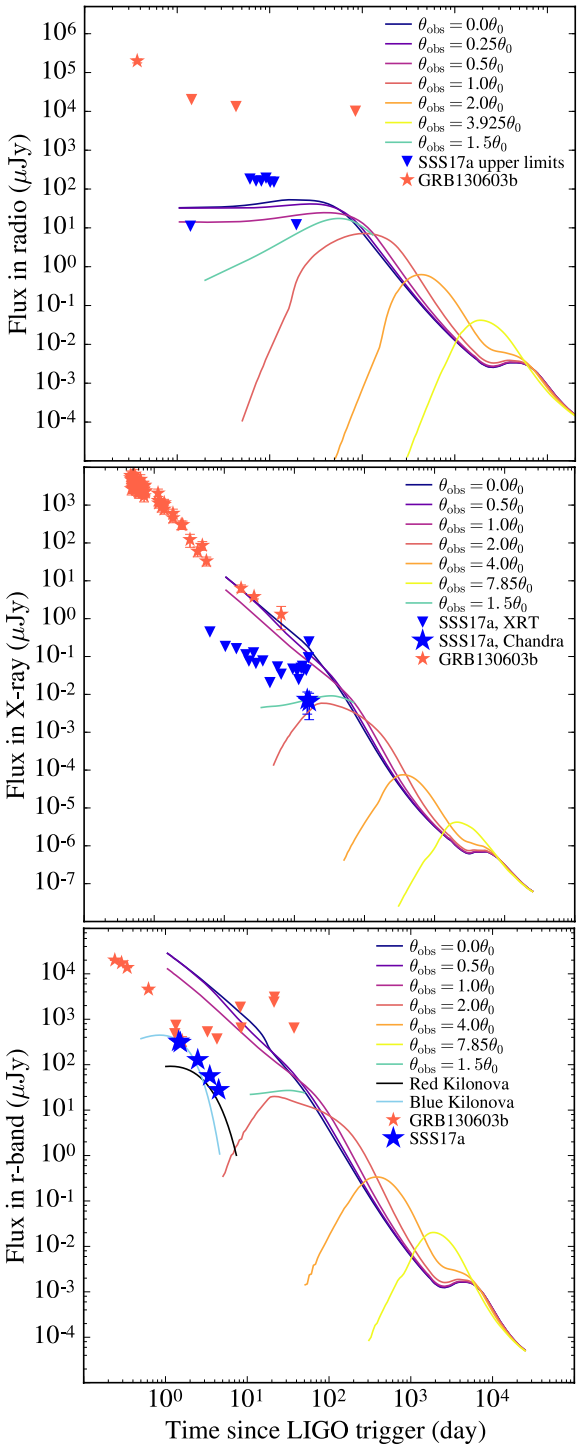


Figure 5. Afterglow emission from a standard off-axis jet (scenario *b* in Figure 1). Light curves are calculated for various viewing angles $\theta_{\rm obs}$ at optical (r-band), radio (6 GHz), and X-rays (7×10^{16} Hz) for a sGRB with standard parameters: $n = 0.3$ cm^{-3}, $E_{\rm K,iso} = 2.5 \times 10^{51}$ erg, $p = 2.8$, $\epsilon_B = 0.002$, $\epsilon_e = 0.02$ and $\xi_N = 1$. The curves presented here are calculated using the models from van Eerten & MacFadyen (2011). Also plotted is the same data and kilonova models shown in Figure 3. The data for GRB 170817a/SSS17a can be reasonably fit by a standard sGRB seen seen at $\theta_{\rm obs} = 1.5\theta_0$, where θ_0=0.2. The on axis model is broadly compatible with the properties of typical sGRBs as illustrated by the comparison with GRB 130603b (Fong et al. 2015).

Kilpatrick et al. 2017 predicts the kinetic ejecta content at sub-relativistic velocities ($v_{\rm ejecta} \approx 0.1c$) to be of the order of a few times 10^{51} erg.

The faint nature of GRB 170817a can be used to argue for the existence of at least two different possibilities for the nature of the sGRB event associated with GW170817, on the basis of different amounts of relativistic energy released during the initial explosion. In this *Letter*, we have examined two concrete alternatives. The first one is based on the premise that GRB 170817a was an intrinsically weak, nearly isotropic explosion and we conclude that current observations are also consistent with this idea (Section 3). In this scenario, the kinetic energy content at mildly relativistic velocities $\Gamma \approx 5$ is estimated to be $\approx 10^{49}$ erg. The second alternative is based on the hypothesis that GRB 170817a was an ordinary GRB observed off-axis, and in this case we conclude that current available data is consistent with an off-axis model in which GRB 170817a was a much more powerful event seen at an angle of about 1.5 times the opening angle of the jet (Section 4). The kinetic energy content at relativistic velocities $\Gamma \approx 10^2$ is thus estimated to be $\approx 10^{50}$ erg after correcting for beaming. Detailed X-ray and radio follow-up observations and polarimetry of GRB 170817a/SSS17a should provide us with stringent constraints on the jet geometry and energetics, as both models make very different predictions. [1] The off-axis model, for example, will be preferred if the X-ray and radio fluxes are observed to increase.

The progenitors of sGRBs have been until now essentially masked by afterglow emission, which is largely featureless synchrotron emission (Nakar 2007). The detection of kilonova emission has clearly established the potential of electromagnetic signatures to shed light on the properties of the ejecta and its composition after merger (Kilpatrick et al. 2017). As we have described, our rationalization of the principal post-merger physical considerations combines some generally accepted principles with some more speculative ingredients (Figure 1). When confronted with observations, it seems to accommodate the gross properties of the electromagnetic radiation (Figures 3 and 5), in addition to the incalculable value of the information that will be gathered from the concurrent gravitational event will provide us with the exciting opportunity to study and test new regimes of physics.

ACKNOWLEDGMENTS

We thank the LIGO/Virgo Collaboration, and all those who have contributed to gravitational wave science for enabling this discovery. We thank J. McIver and B. Mockler, and the anonymous referee. We would like to thank I. Thompson, J. Mulchaey (Carnegie), L. Infante and the entire Las Campanas staff. We thank K. Alexander, W-F. Fong, R. Margutti , the EuroVLBI team, the INTEGRAL team, the Chandra team and the Fermi-GBM team for granting permission to use their data. We thank the University of Copenhagen, DARK Cosmology Centre, and the Niels Bohr International Academy for hosting D.A.C., R.J.F., A.M.B., E.R., and M.R.S. during the discovery of GW170817/SSS17a. R.J.F., A.M.B., and E.R. were participating in the Kavli Summer Program in Astrophysics, "Astrophysics with gravitational wave detections." This program was supported by the the Kavli Foundation, Danish National Research Foundation, the Niels Bohr International Academy, and the DARK Cosmology Centre. The UCSC group is supported in part by NSF grant AST–1518052, the Gordon & Betty Moore Foundation, the Heising-Simons Foundation, generous donations from many individuals through a UCSC Giving Day grant, and from fellowships from the Alfred P. Sloan Foundation (R.J.F), the David and Lucile Packard Foundation (R.J.F. and E.R.) and the Niels Bohr Professorship from the DNRF (E.R.). A.M.B. acknowledges support from a UCMEXUS-CONACYT Doctoral Fellowship. W.H.L. is supported in part by UNAM-PAPIIT grant IG100317.

Support for this work was provided by NASA through Hubble Fellowship grant HST–HF–51373.001 awarded by the Space Telescope Science Institute, which is operated by the Association of Universities for Research in Astronomy, Inc., for NASA, under contract NAS5–26555. This paper includes data gathered with the 6.5 meter Magellan Telescopes located at Las Campanas Observatory, Chile. This research has made use of the NASA/IPAC Extragalactic Database (NED) which is operated by the Jet Propulsion Laboratory, California Institute of Technology, under contract with the National Aeronautics and Space Administration. Based on observations made with the NASA/ESA Hubble Space Telescope, obtained from the Data Archive at the Space Telescope Science Institute, which is operated by the Association of Universities for Research in Astronomy, Inc., under NASA contract NAS 5–26555. These observations are associated with programs GO–14840.

REFERENCES

[1] It should be noted that there is a disagreement about the possible detection of a radio afterglow at t =17-19 days (GROWTH 2017; Alexander et al. 2017). If confirmed both models presented here can be slightly modified to provide a reasonable description of the data at this specific epoch.

Abbott, B. P., Abbott, R., Abbott, T. D., et al. 2016, ApJL, 832, L21
Abbott et al. 2017a, Accepted in PRL
—. 2017b, in prep
Alexander et al. 2017, submitted
Barnes, J., & Kasen, D. 2013, ApJ, 775, 18
Baumgarte, T. W., Shapiro, S. L., & Shibata, M. 2000, ApJL, 528, L29
Behroozi, P. S., Ramirez-Ruiz, E., & Fryer, C. L. 2014, ApJ, 792, 123
Berger, E. 2014, ARA&A, 52, 43
Bloom, J. S., Kulkarni, S. R., Harrison, F., et al. 1998, ApJL, 506, L105
Champion, D. J., Lorimer, D. R., McLaughlin, M. A., et al. 2004, MNRAS, 350, L61
Coulter et al. 2017, submitted to Science
D'Avanzo, P., Salvaterra, R., Bernardini, M. G., et al. 2014, MNRAS, 442, 2342
Drout et al. 2017, submitted to Science
Duez, M. D., Liu, Y. T., Shapiro, S. L., Shibata, M., & Stephens, B. C. 2006, Physical Review Letters, 96, 031101
Eichler, D., Livio, M., Piran, T., & Schramm, D. N. 1989, Nature, 340, 126
Faber, J. A., & Rasio, F. A. 2012, Living Reviews in Relativity, 15, 8
Fong, W., Berger, E., Margutti, R., & Zauderer, B. A. 2015, ApJ, 815, 102
Freiburghaus, C., Rosswog, S., & Thielemann, F.-K. 1999, ApJL, 525, L121
Gehrels, N., Ramirez-Ruiz, E., & Fox, D. B. 2009, ARA&A, 47, 567
Granot, J., Panaitescu, A., Kumar, P., & Woosley, S. E. 2002, ApJL, 570, L61
GROWTH. 2017, GRB Coordinates Network, 21815
Guetta, D., & Piran, T. 2006, A&A, 453, 823
Haggard et al. 2017, in preparation
Hulse, R. A., & Taylor, J. H. 1975, ApJL, 195, L51
Just, O., Obergaulinger, M., Janka, H.-T., Bauswein, A., & Schwarz, N. 2016, ApJL, 816, L30
Kaneko, Y., Ramirez-Ruiz, E., Granot, J., et al. 2007, ApJ, 654, 385
Kasen, D., Badnell, N. R., & Barnes, J. 2013, ApJ, 774, 25
Kasen, D., Fernández, R., & Metzger, B. D. 2015, MNRAS, 450, 1777
Kasen et al. 2017, submitted to Nature
Kilpatrick et al. 2017, submitted to Science
Kluźniak, W., & Lee, W. H. 1998, ApJL, 494, L53
Kouveliotou, C., Meegan, C. A., Fishman, G. J., et al. 1993, ApJL, 413, L101
Kumar, P., & Zhang, B. 2015, PhR, 561, 1
Lee, W. H., & Ramirez-Ruiz, E. 2007, New Journal of Physics, 9, 17
Leventis, K., van Eerten, H. J., Meliani, Z., & Wijers, R. A. M. J. 2012, MNRAS, 427, 1329
Li, L.-X., & Paczyński, B. 1998, ApJL, 507, L59
LIGO/Virgo collaboration. 2017, GRB Coordinates Network, 21509
LVC, GBM, INTEGRAL. 2017, in preparation
Metzger, B. D. 2017, Living Reviews in Relativity, 20, 3
Metzger, B. D., & Zivancev, C. 2016, MNRAS, 461, 4435
Metzger, B. D., Martínez-Pinedo, G., Darbha, S., et al. 2010, MNRAS, 406, 2650
Murguia-Berthier, A., Montes, G., Ramirez-Ruiz, E., De Colle, F., & Lee, W. H. 2014, ApJL, 788, L8
Murguia-Berthier, A., Ramirez-Ruiz, E., Montes, G., et al. 2017, ApJL, 835, L34
Nagakura, H., Hotokezaka, K., Sekiguchi, Y., Shibata, M., & Ioka, K. 2014, ApJL, 784, L28
Nakar, E. 2007, PhR, 442, 166
Narayan, R., Paczynski, B., & Piran, T. 1992, ApJL, 395, L83
Norris, J. P., & Bonnell, J. T. 2006, ApJ, 643, 266
Paciesas, W. S., Meegan, C. A., Pendleton, G. N., et al. 1999, ApJS, 122, 465
Paczynski, B. 1986, ApJL, 308, L43
Palmer, D. M., Barthelmy, S., Gehrels, N., et al. 2005, Nature, 434, 1107
Pan et al. 2017, submitted to ApJL
Perego, A., Rosswog, S., Cabezón, R. M., et al. 2014, MNRAS, 443, 3134
Piran, T. 2004, Reviews of Modern Physics, 76, 1143
Piro, A. L., Giacomazzo, B., & Perna, R. 2017, ApJL, 844, L19
Ramirez-Ruiz, E., Granot, J., Kouveliotou, C., et al. 2005, ApJL, 625, L91
Rees, M. J., & Meszaros, P. 1992, MNRAS, 258, 41P
Rezzolla, L., Giacomazzo, B., Baiotti, L., et al. 2011, ApJL, 732, L6
Rezzolla, L., & Kumar, P. 2015, ApJ, 802, 95
Roberts, L. F., Kasen, D., Lee, W. H., & Ramirez-Ruiz, E. 2011, ApJL, 736, L21
Rosswog, S. 2005, ApJ, 634, 1202
Rosswog, S., & Ramirez-Ruiz, E. 2002, MNRAS, 336, L7
—. 2003, MNRAS, 343, L36
Savchenko et al. 2017, under review in ApJL
Shappee et al. 2017, submitted to Science
Shen, S., Cooke, R. J., Ramirez-Ruiz, E., et al. 2015, ApJ, 807, 115
Siebert et al. 2017, submitted to ApJL
Siegel, D. M., Ciolfi, R., & Rezzolla, L. 2014, ApJL, 785, L6
Tsutsui, R., Yonetoku, D., Nakamura, T., Takahashi, K., & Morihara, Y. 2013, MNRAS, 431, 1398
van Eerten, H. J., & MacFadyen, A. I. 2011, ApJL, 733, L37
Woosley, S. E., & Bloom, J. S. 2006, ARA&A, 44, 507